Supplementary Material (ESI) for *PCCP*

Electronic Supplementary Information for:

Crystallographic Structure Refinement with Quadrupolar Nuclei: a Combined Solid-State NMR and GIPAW DFT Example Using $MgBr_2$

Cory M. Widdifield and David L. Bryce*

* *Author to whom correspondence is to be addressed: Department of Chemistry and Centre for Catalysis Research and Innovation, University of Ottawa, 10 Marie Curie Pvt., Ottawa, Ontario, Canada. Tel: +1 613 562 5800 ext 2018; Fax: +1 613 562 5170. E-mail: dbryce@uottawa.ca.*

Supplementary Material (ESI) for *PCCP*

Table of Contents

Supplementary Material (ESI) for *PCCP*

Full Experimental

Sample Preparation.

$MgBr_2$ (98%) was purchased from Aldrich and subjected to SSNMR and pXRD measurements without modification. $MgBr_2$ is hygroscopic and was therefore stored under a dry nitrogen or argon atmosphere to minimize exposure to water. For all SSNMR experiments, the sample was powdered and tightly packed into a 4 mm MAS rotor while under either dry nitrogen or argon. For pXRD experiments, the sample preparation was carried out under dry N_2: the sample was packed into a 1.0 mm (o.d.) thin wall (10 micron) borosilicate glass capillary, which was then sealed with epoxy and sent for external analysis at Université de Montréal.

Solid-state NMR.

Magnesium-25 and $^{79/81}$Br SSNMR spectra were acquired at the University of Ottawa using a wide bore (89 mm) Bruker *Avance* spectrometer operating at $\mathbf{B}_0$ = 11.75 T ($\nu(^1H)$ = 500.13 MHz) and at the National Ultrahigh-field NMR Facility for Solids in Ottawa using a standard bore (54 mm) Bruker *AvanceII* spectrometer operating at $\mathbf{B}_0$ = 21.1 T ($\nu(^1H)$ = 900.21 MHz)). At 11.75 T, all experiments used a Bruker 4 mm triple-resonance MAS probe ($\nu(^{81}Br)$ = 135.075 MHz/$\nu(^{79}Br)$ = 125.309 MHz/$\nu(^{25}Mg)$ = 30.615 MHz). At the Ultrahigh-field NMR Facility, all experiments used a Bruker 4 mm double-resonance MAS probe ($\nu(^{81}Br)$ = 243.093 MHz/$\nu(^{79}Br)$ = 225.519 MHz/$\nu(^{25}Mg)$ = 55.098 MHz).

Br-79/81 SSNMR signals were primarily acquired using a Solomon echo pulse sequence[1,2] (i.e., $\pi/2 - \tau_1 - \pi/2 - \tau_2 - acq$) and the phase cycling suggested by Kunwar *et al*.[3] The quadrupolar Carr-Purcell Meiboom-Gill (QCPMG) pulse sequence was also used at $\mathbf{B}_0$ = 11.75 T to enhance the bromine NMR signal and thus reduce experiment times.[4-6] The QCPMG

sequence was also used at both fields to estimate T_2 values. The estimated T_2 values were such that whole-echo data acquisition could be carried out, thereby increasing the sensitivity of the Solomon echo experiment by $\sqrt{2}$. Detailed $^{79/81}$Br Solomon echo ("echo") and QCPMG pulse sequence parameters can be found in Table S1. Bromine chemical shifts and $\pi/2$ pulse widths were determined using the bromine NMR signal of powdered solid KBr (δ_{Br}(KBr(s)) = 0.0 ppm). As KBr is a cubic salt, central-transition selective pulse widths used for $MgBr_2$ were scaled by $1/(I + 1/2) = 1/2$. For the $^{79/81}$Br SSNMR experiments carried out at 11.75 T, variable-offset data acquisition was required. Typical offsets were 250 kHz to 300 kHz for Solomon echo experiments, while QCPMG experiments used offsets ranging from 87.8 to 95.9 kHz. Each "sub-spectrum" was processed as usual and combined in the frequency-domain by co-adding the sub-spectra.

Mg-25 SSNMR signals were acquired using a "pulse-acquire" sequence under MAS conditions. Detailed ^{25}Mg SSNMR acquisition parameters are listed in Table S1. Magnesium chemical shifts and $\pi/2$ pulse widths were determined using the ^{25}Mg NMR signal of 1.0 M aqueous $MgCl_2$ (δ_{Mg}(1.0 M $MgCl_2$(aq) = 0.0 ppm). All solid state ^{25}Mg pulse widths were scaled by $1/(I + 1/2) = 1/3$.

Powder X-ray Diffraction.

Experiments were carried out using an APEX-II single-crystal diffractometer using MoKα radiation (λ = 0.7093 Å) equipped with a CCD detector. Data were collected over the range $4.96° < 2\theta < 46.78°$ and clearly demonstrate that the $MgBr_2$ sample had not formed the hexahydrate pseudopolymorph (Figure S3).

Computational Details.

Gauge-including projector-augmented-wave (GIPAW) Kohn-Sham density functional theory (DFT) computations were carried out using the Materials Studio CASTEP-NMR routine,[7-9] and run under version 4.1 of CASTEP.[10] Both magnesium and bromine on-the-fly pseudopotential files were obtained directly from Accelrys Inc. (San Diego, CA). Geometry optimizations, as well as NMR magnetic shielding and EFG tensor calculations were performed using the Perdew-Burke-Ernzerhof (PBE) exchange-correlation functional[11,12] which uses the generalized gradient approximation (GGA). Selected computations were also carried out using the PW91 functional,[13-17] yielding similar computed values (Tables S2 to S4). NMR parameter convergence was tested by varying both the Monkhorst-Pack[18] *k*-point sampling of the Brillouin zone, as well as the plane wave basis set energy cutoff (Figures S4 to S6). All calculations used the 'precise' setting, as defined by Materials Studio, for the fast-Fourier transform (FFT) grid (used to transform between real and reciprocal spaces). It was found that both the system energy and relevant NMR parameters were satisfactorily converged at E_{cut} = 400 eV (~29.4 Ry), using a 10 × 10 × 6 *k*-point grid (i.e., $E_{1200} - E_{400}$ = –0.35 kJ mol^{-1}; $C_Q(^{81}Br_{1200}) - C_Q(^{81}Br_{400})$ = 0.02 MHz; $\delta_{iso}(^{81}Br_{1200}) - \delta_{iso}(^{81}Br_{400})$ = 0.20 ppm, where the subscripts denote the plane wave basis set energy cutoff). Usage of a 15 × 15 × 8 *k*-point grid, relative to a 10 × 10 × 6 *k*-point grid (using E_{cut} = 610 eV) resulted in no change in the bromine EFG tensor parameters and a ~0.1 ppm change in the calculated isotropic shielding values. The 'fully optimized' geometry, a 400 eV plane wave basis set energy cutoff and a 10 × 10 × 6 *k*-point grid were used for computations that simulated the movement of the bromine atoms parallel to the *c* unit cell direction (Figures 3 and S7). To convert calculated magnetic shielding tensor eigenvalues into isotropic chemical shielding values, the following procedure was used: the bromine σ_{iso} value for the reference

compound KBr, ($\sigma_{iso,\ ref}$) was determined using an 800 eV plane wave basis set energy cutoff and a 6 × 6 × 6 *k*-point grid using the same exchange-correlation functional (i.e., either PBE or PW91) as $MgBr_2$. Then, the following formula was used: $\delta_{iso} = (\sigma_{iso,\ ref} - \sigma_{iso})/(1 - \sigma_{iso,\ ref})$, where σ_{iso} is the isotropic bromine magnetic shielding value for $MgBr_2$ and δ_{iso} is the isotropic bromine chemical shift value for $MgBr_2$.

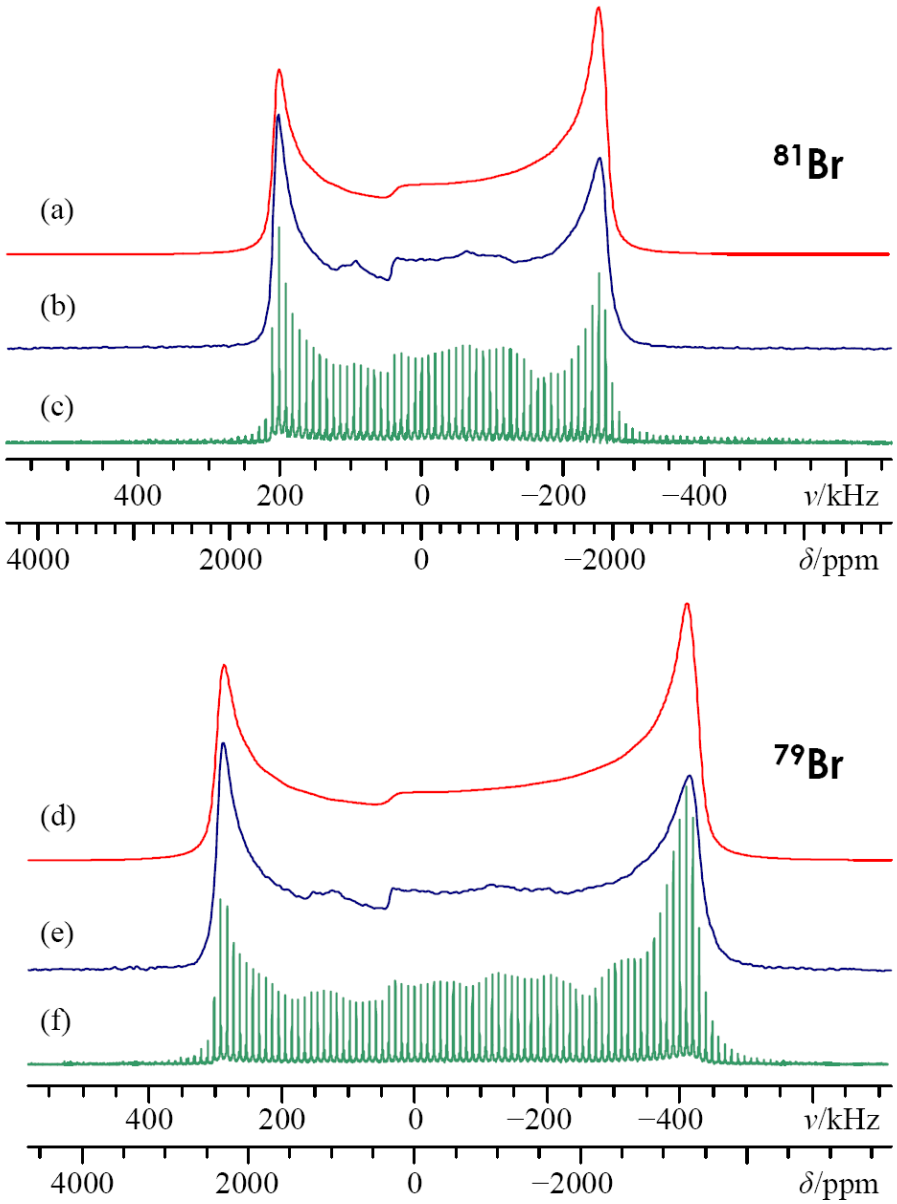

Figure S1. Experimental Solomon echo ^{81}Br (b) and ^{79}Br (e), as well as experimental QCPMG ^{81}Br (c) and ^{79}Br (f) SSNMR spectra of $MgBr_2$ under static conditions at $\mathbf{B}_0$ = 11.75 T. Corresponding analytical lineshape simulations are given in (a) and (d). We attribute small discrepancies between the experimental and simulated lineshapes to the neglect of a small amount (< 50 ppm) of CSA and trace impurities (i.e., hydrates) in the sample.

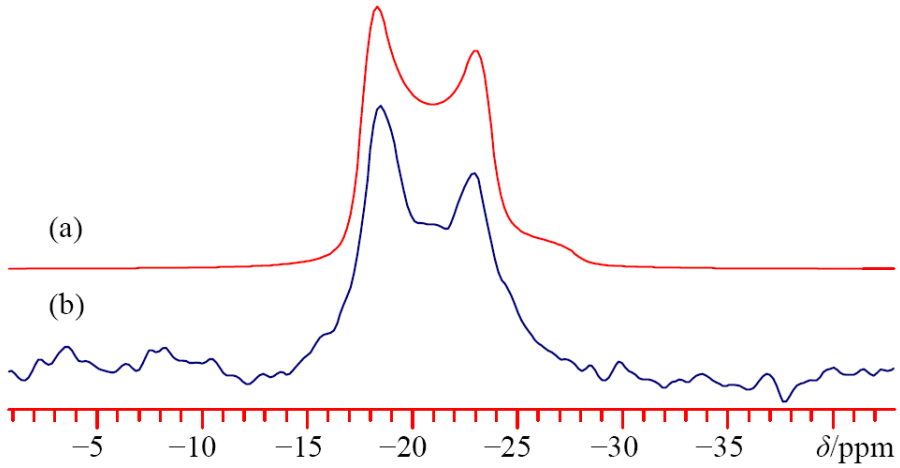

Figure S2. Experimental ^{25}Mg (b) SSNMR spectrum under MAS conditions (ν_{rot} = 5 kHz) and $\mathbf{B}_0$ = 11.75 T. Corresponding analytical lineshape simulation is given in (a).

Table S1. Detailed SSNMR experimental acquisition parameters[a]

$\mathbf{B}_0$ / T	^{A}X	Window / kHz	Points[b]	$\pi/2$ / μs	Scans	Pulse delay / s	τ_1/τ_2 / μs	Details
11.75	^{81}Br	625	26598	1.7	1152	0.4	60[c]	static; QCPMG; 201 MG loops; 11 pieces; offset = 95.9 kHz
11.75	^{79}Br	714.286	30118	1.8	1920	0.45	60[c]	static; QCPMG; 203 MG loops; 11 pieces; offset = 87.8 kHz
11.75	^{81}Br	2000	2048	1.2	12000	0.4	250/10	static; Solomon echo; 3 pieces; offset = 300 kHz
11.75	^{79}Br	2000	2048	1.1	12000	0.4	250/10	static; Solomon echo; 5 pieces; offset = 300 kHz
21.1	^{81}Br	1000	2048	1.0	2048	0.6	300/10	static; Solomon echo; 1 piece
21.1	^{79}Br	2000	4096	1.2	2048	0.6	300/10	static; Solomon echo; 1 piece
11.75	^{25}Mg	10	2048	4.5	560	90	—	MAS; pulse-acq; ν_{rot} = 5 kHz
21.1	^{25}Mg	10	4096	4.2	104	60	—	MAS; pulse-acq; ν_{rot} = 5 kHz

[a] all experiments were carried out at room temperature.
[b] the number of complex time-domain data points acquired.
[c] all four τ values were set to 60 μs.

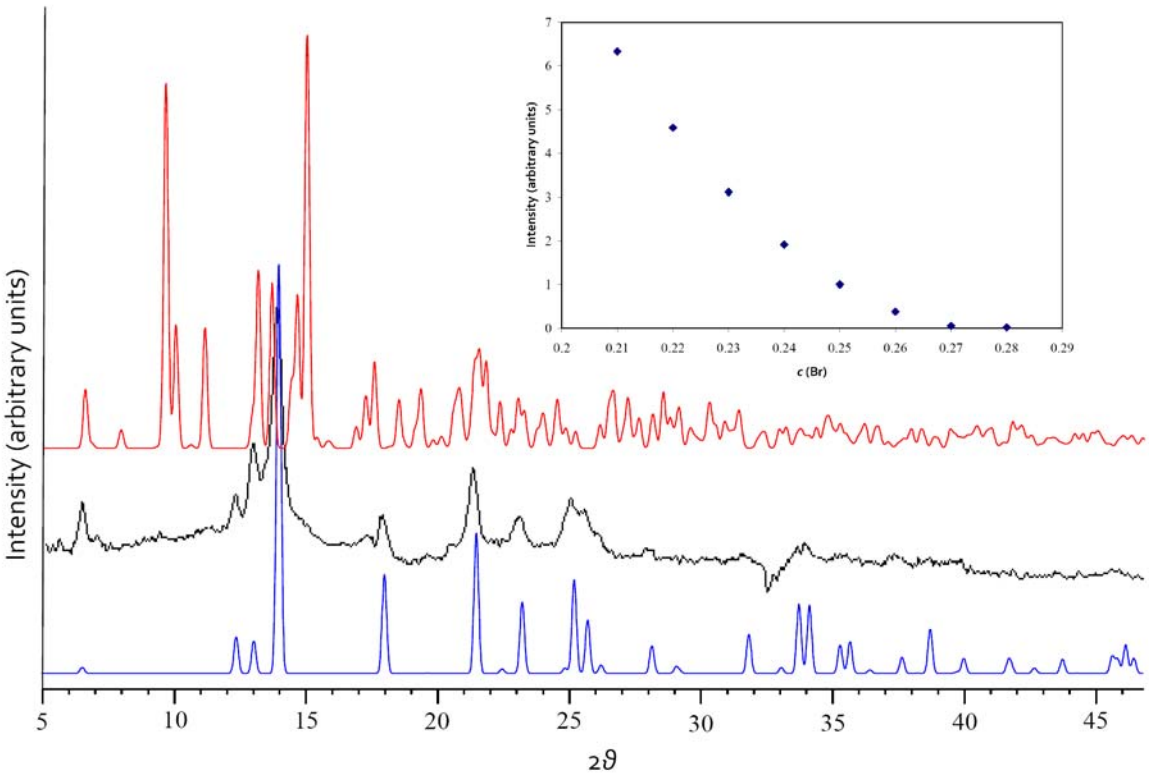

Figure S3. Experimental powder XRD patterns of the sample used for SSNMR experimentation (middle) agrees qualitatively with the database entry for $MgBr_2$ (bottom). The agreement is quite poor however, between the experimental pXRD pattern and the database entry for $MgBr_2 \cdot 6H_2O$ (top). It is concluded therefore that SSNMR experiments had indeed been carried out on anhydrous $MgBr_2$. The dip around $2\theta = 32°$ is due to a defect in the detector. As noted in the manuscript, the pXRD data acquired here agree with our main conclusions regarding the modified structure of $MgBr_2$. This is explained below. The peaks which occur at $2\theta = 6.32°$ and 12.84º belong to (001) and (002). By a simple application of Bragg's Law, one arrives at c values of 6.43 Å and 6.34 Å, both of which are greater than the currently accepted value (6.26 Å), in agreement with our conclusions. As well, it should be noted that the intensity of the (001) peak is highly dependent upon the c position of the bromine ions (see the inset plot of the intensity of the (001) peak versus c(Br) for a constant unit cell; note that the intensity of the point where c(Br) = 0.25 has been arbitrarily normalized to unity). Working within the space group of the accepted structure, as the value of c(Br) increases, the intensity of the (001) peak should decrease, becoming vanishingly small at values above c(Br) = 0.26. Therefore, based upon only the pXRD data, if c(Br) = 0.25, then the intensity of the (001) peak would be very small (perhaps under our detection limits). As well, if one changes c(Br) to be progressively less than 0.25 (as in the inset), the intensity of the (001) peak systematically increases. Hence, the observed pXRD data are also in support of a c(Br) value that is decidedly below the previously accepted value of 0.25.

Table S2. Detailed GIPAW DFT computed NMR parameters based on the 1929 pXRD structure[a]

Method	Energy / eV	V_{11} / a.u.	V_{22} / a.u.	V_{33} / a.u.	C_Q[b] / MHz	η_Q	σ_{11} / ppm	σ_{22} / ppm	σ_{33} / ppm	Ω[c] / ppm	κ	δ_{iso} / ppm
Bromine-81 NMR parameters												
PBE	−2009.410406	0.0316	0.0316	−0.0633	−3.90	0.000	2264.05	2279.96	2280.09	16.03	−0.985	353.11
PW91	−2012.541456	0.0335	0.0335	−0.0671	−4.13	0.000	2265.97	2282.48	2282.60	16.64	−0.985	350.06
Magnesium-25 NMR Parameters												
PBE	−2009.410406	0.0370	0.0370	−0.0741	−3.47	0.000	549.75	554.43	554.46	4.71	−0.987	—
PW91	−2012.541456	0.0373	0.0373	−0.0747	−3.50	0.000	550.38	555.05	555.07	4.69	−0.990	—

[a] All computed values contained within this table used a 1200 eV basis set energy cutoff and a 10 × 10 × 6 *k*-point grid. The geometry used can be found in Table S5.
[b] The electric-field gradient (EFG) tensor is traceless and the eigenvalues are defined such that $|V_{11}| \le |V_{22}| \le |V_{33}|$. $C_Q = eQV_{33}/h$; $\eta_Q = (V_{11} - V_{22})/V_{33}$; $V_{33} = eq$; $q = 1.602176487 \times 10^{-19}$ C; $h = 6.62606896 \times 10^{-34}$ J s; $Q(^{25}\text{Mg}) = 1.994 \times 10^{-29}$ m^2 ; $Q(^{79}\text{Br}) = 3.13 \times 10^{-29}$ m^2; $Q(^{81}\text{Br}) = 2.62 \times 10^{-29}$ m^2;. All EFG tensor eigenvalues are reported in atomic units (a.u.). To convert EFG tensor eigenvalues to MHz, conversion factors of 61.56077 MHz/a.u. and 46.85197 MHz/a.u. were used for ^{81}Br and ^{25}Mg, respectively, and is based on the definition that the unit EFG in a.u. is $9.71736166 \times 10^{21}$ J C^{-1} m^{-2}.
[c] The magnetic shielding tensor carries a trace and the eigenvalues are defined such that $\sigma_{11} \le \sigma_{22} \le \sigma_{33}$. $\sigma_{iso} = (\sigma_{11} + \sigma_{22} + \sigma_{33})/3$; $\Omega = \sigma_{33} - \sigma_{11}$; $\kappa = 3(\sigma_{iso} - \sigma_{22})/\Omega$.

Table S3. Detailed GIPAW DFT computed NMR parameters based on optimizing *c*(Br) only[a]

Method	Energy / eV	V_{11} / a.u.	V_{22} / a.u.	V_{33} / a.u.	C_Q / MHz	η_Q	σ_{11} / ppm	σ_{22} / ppm	σ_{33} / ppm	Ω / ppm	κ	δ_{iso} / ppm
Bromine-81 NMR parameters												
PBE	−2009.429912	0.1209	0.1209	−0.2418	−14.89	0.000	2264.26	2293.54	2293.66	29.41	−0.992	343.97
PW91	−2012.561001	0.1229	0.1229	−0.2459	−15.14	0.000	2266.09	2295.96	2296.09	30.00	−0.992	341.01
Magnesium-25 NMR Parameters												
PBE	−2009.429912	0.0318	0.0318	−0.0635	−2.98	0.000	547.92	552.92	552.97	5.05	−0.983	—
PW91	−2012.561001	0.0321	0.0321	−0.0643	−3.01	0.000	548.52	553.48	553.52	5.00	−0.982	—

[a] All computed values contained within this table used a 1200 eV basis set energy cutoff and a 10 × 10 × 6 *k*-point grid. Optimized geometry can be found in Table S5.

Table S4. Detailed GIPAW DFT computed NMR parameters based on a fully optimized (cell and atomic positions) structure[a]

Method	Energy / eV	V_{11} / a.u.	V_{22} / a.u.	V_{33} / a.u.	C_Q / MHz	η_Q	σ_{11} / ppm	σ_{22} / ppm	σ_{33} / ppm	Ω / ppm	κ	δ_{iso} / ppm
Bromine-81 NMR parameters												
PBE	−2009.481718	0.1771	0.1771	−0.3543	−21.81	0.000	2271.29	2324.59	2324.69	53.40	−0.996	320.88
PW91	−2012.614200	0.1823	0.1823	−0.3647	−22.45	0.000	2273.93	2328.14	2328.24	54.31	−0.996	316.89
Magnesium-25 NMR Parameters												
PBE	−2009.481718	0.0292	0.0292	−0.0584	−2.74	0.000	549.97	555.78	555.84	5.86	−0.982	—
PW91	−2012.614200	0.0296	0.0296	−0.0593	−2.78	0.000	550.74	556.49	556.53	5.78	−0.989	—

[a] All computed values contained within this table used a 1200 eV basis set energy cutoff and a 10 × 10 × 6 *k*-point grid. Fully optimized geometry can be found in Table S5.

Table S5. $MgBr_2$ crystal structure parameters used for computations[a]

Atom	Wyckoff position	X[b]	Y	Z
previously accepted pXRD structure[c]				
Mg	1a	0.0000	0.0000	0.0000
Br	2d	0.3333	0.6667	0.2500
'optimized c(Br)' (i.e., fixed cell) GIPAW DFT optimized structure[c]				
Mg	1a	0.0000	0.0000	0.0000
Br	2d	0.3333	0.6667	0.2424
'fully optimized' GIPAW DFT optimized structure[d]				
Mg	1a	0.0000	0.0000	0.0000
Br	2d	0.3333	0.6667	0.2125

[a] The 'fixed cell' and 'fully optimized' geometries were determined used the PBE method (defined above), a 800 eV basis set energy cutoff and a 10 × 10 × 6 *k*-point grid.
[b] In fractional unit cell coordinates.
[c] Observed values: $a = b = 3.81$ Å; $c = 6.26$ Å.
[d] Optimized values: $a = b = 3.887$ Å; $c = 7.108$ Å.

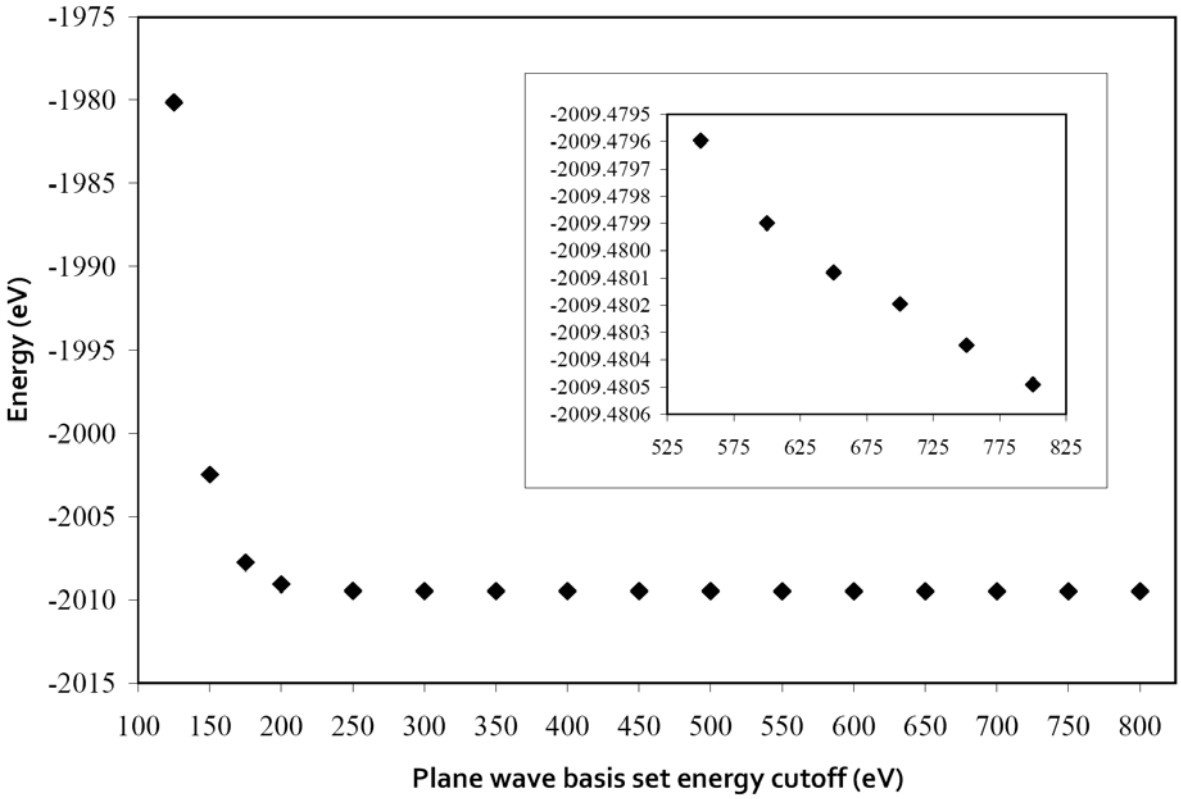

Figure S4. $MgBr_2$ energy versus plane wave basis set energy cutoff clearly demonstrates convergence with respect to energy. Computations used the GIPAW DFT fully optimized geometry.

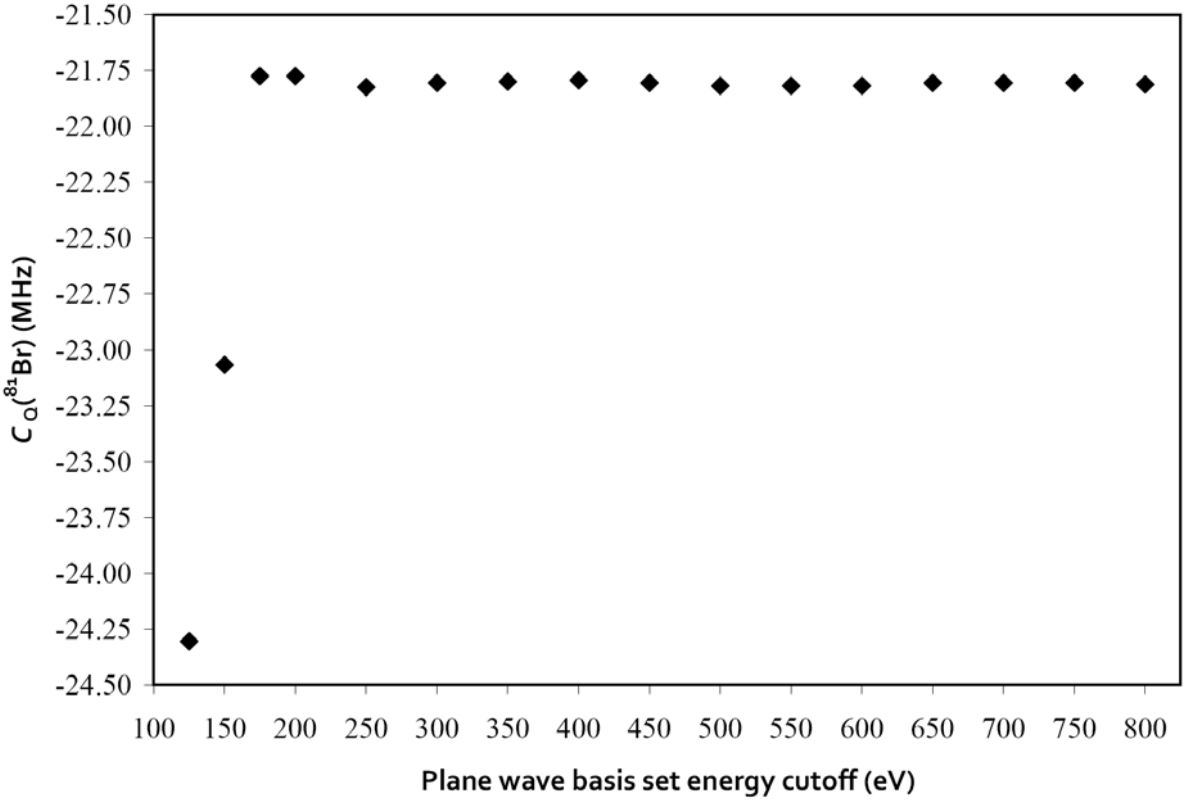

Figure S5. $C_Q(^{81}Br)$ of $MgBr_2$ versus the plane wave basis set energy cutoff clearly demonstrates convergence with respect to this parameter. Computations used the GIPAW DFT fully optimized geometry.

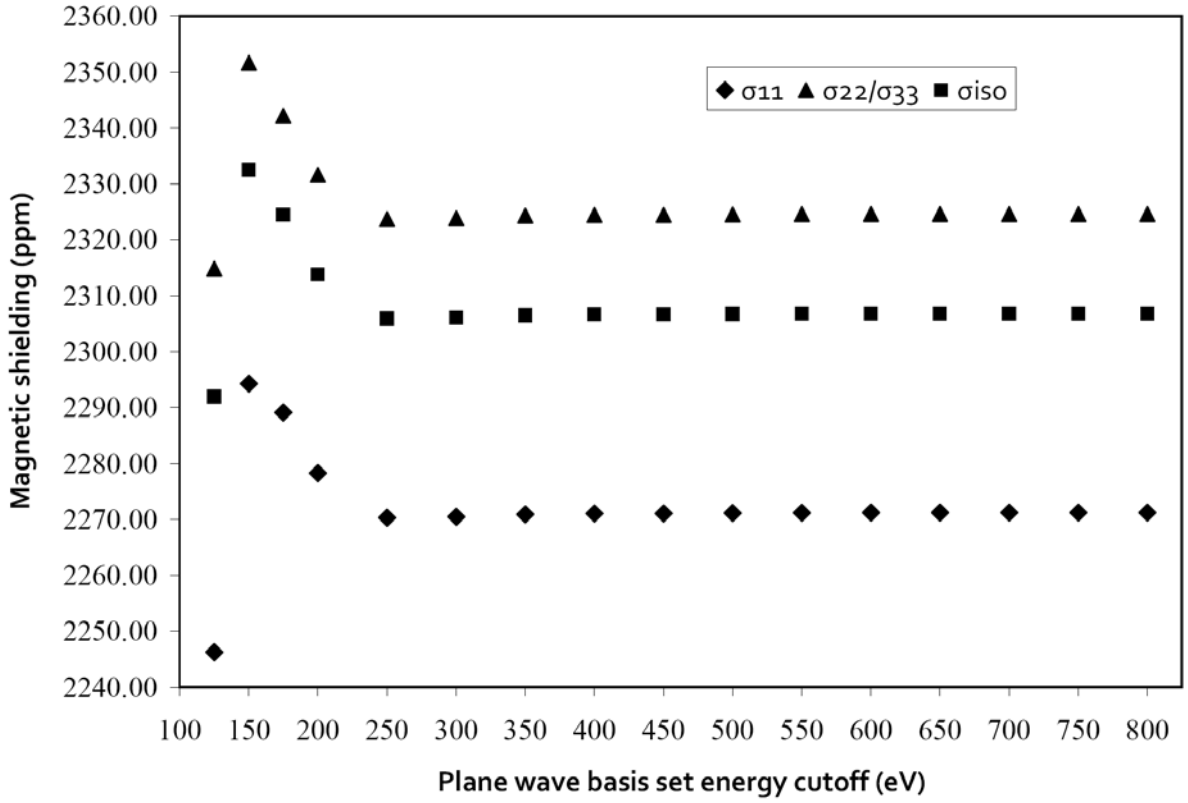

Figure S6. Bromine magnetic shielding parameters for $MgBr_2$ versus the plane wave basis set energy cutoff clearly demonstrates convergence with respect to these parameters. Computations used the GIPAW DFT fully optimized geometry.

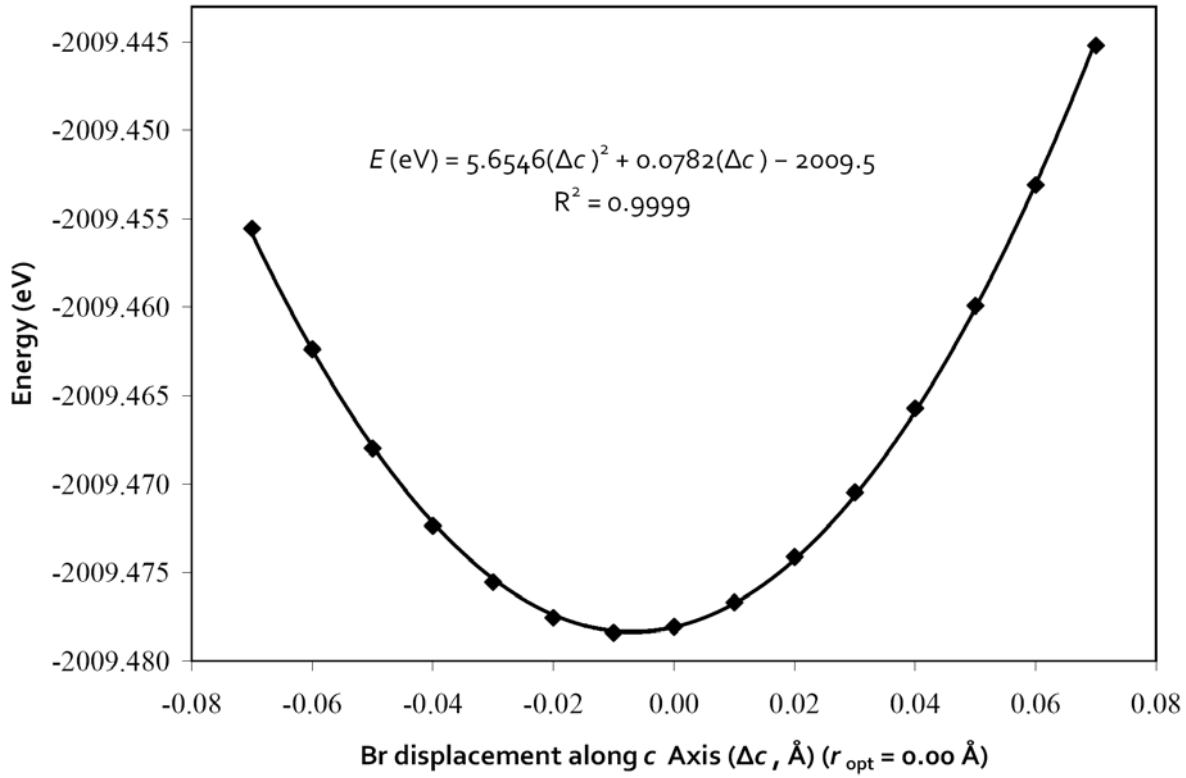

Figure S7. Plot of $MgBr_2$ energy versus the displacement of the bromine atom parallel to the *c* unit cell axis. The optimized position (r_{opt} = 0.00 Å) is from the GIPAW DFT fully optimized geometry.

ESI References

1 I. Solomon, *Phys. Rev.,* 1958, **110,** 61.

2 I. D. Weisman and L. H. Bennett, *Phys. Rev.,* 1969, **181,** 1341.

3 A. C. Kunwar, G. L. Turner and E. Oldfield, *J. Magn. Reson.,* 1986, **69,** 124.

4 H. Y. Carr and E. M. Purcell, *Phys. Rev.,* 1954, **94,** 630.

5 S. Meiboom and D. Gill, *Rev. Sci. Instrum.,* 1958, **29,** 688.

6 F. H. Larsen, H. J. Jakobsen, P. D. Ellis and N. C. Nielsen, *J. Phys. Chem. A,* 1997, **101,** 8597.

7 C. J. Pickard and F. Mauri, *Phys. Rev. B,* 2001, **63,** 245101-1.

8 J. R. Yates, C. J. Pickard and F. Mauri, *Phys. Rev. B,* 2007, **76,** 024401-1.

9 M. Profeta, F. Mauri and C. J. Pickard, *J. Am. Chem. Soc.,* 2003, **125,** 541.

10 S. J. Clark, M. D. Segall, C. J. Pickard, P. J. Hasnip, M. I. J. Probert, K. Refson and M. C. Payne, *Z. Kristallogr.,* 2005, **220,** 567.

11 J. P. Perdew, K. Burke and M. Ernzerhof, *Phys. Rev. Lett.,* 1996, **77,** 3865.

12 J. P. Perdew, K. Burke and M. Ernzerhof, *Phys. Rev. Lett.,* 1997, **78,** 1396.

13 K. Burke, J. P. Perdew and Y. Wang, *Electric Density Functional Theory: Recent Progress and New Directions,* ed. J. F. Dobson, G. Vignale and M. P. Das. 1998.

14 J. P. Perdew, *Electronic Structure of Solids '91,* ed. P. Ziesche and H. Eschrig. 1991. p11.

15 J. P. Perdew, J. A. Chevary, S. H. Vosko, K. A. Jackson, M. R. Pederson, D. J. Singh and C. Fiolhais, *Phys. Rev. B,* 1992, **46,** 6671.

16 J. P. Perdew, J. A. Chevary, S. H. Vosko, K. A. Jackson, M. R. Pederson, D. J. Singh and C. Fiolhais, *Phys. Rev. B,* 1993, **48,** 4978.

17 J. P. Perdew, K. Burke and Y. Wang, *Phys. Rev. B,* 1996, **54,** 16533.

18 H. J. Monkhorst and J. D. Pack, *Phys. Rev. B,* 1976, **13,** 5188.